J. Fluid Mech. (1966), *vol.* 24, *part* 4, *pp.* 781–800
Printed in Great Britain

On the flow due to a rotating disk

By EDWARD R. BENTON†
National Center for Atmospheric Research, Boulder, Colorado

(Received 14 May 1965 and in revised form 15 August 1965)

The von Kármán (1921) rotating disk problem is extended to the case of flow started impulsively from rest; also, the steady-state problem is solved to a higher degree of accuracy than previously by a simple analytical-numerical method which avoids the matching difficulties in Cochran's (1934) well-known solution. Exact representations of the non-steady velocity field and pressure are given by suitable power-series expansions in the angle of rotation, Ωt, with coefficients that are functions of a similarity variable. The first four equations for velocity coefficient functions are solved exactly in closed form, and the next six by numerical integration. This gives four terms in the series for the primary flow and three terms in each series for the secondary flow.

The results indicate that the asymptotic steady state is approached after about 2 radians of the disk's motion and that it can be approximately obtained from the initial-value, time-dependent analysis. Furthermore, the non-steady flow has three phases, the first two of which are accurately and fully described with the terms computed. During the first-half radian (phase 1), the velocity field is essentially similar in time, with boundary-layer thickening the only significant effect. For $0{\cdot}5 \lesssim \Omega t \lesssim 1{\cdot}5$ (phase 2), boundary-layer growth continues at a slower rate, but simultaneously the velocity profiles adjust towards the shape of the ultimate steady-state profiles. At about $\Omega t = 1{\cdot}5$, some flow quantities overshoot the steady-state values by small amounts. In analogy with the 'Greenspan–Howard problem' (1963) it is believed that the third phase ($\Omega t > 1{\cdot}5$) consists of a small amplitude decaying oscillation about the steady-state solution.

1. Introduction

The direct analytical approach for most steady-state flow problems is especially difficult because of the essential non-linearity of the governing differential equations in this case. Recourse is nearly always made to approximate methods, which are only satisfactory in varying degrees. A potentially powerful alternative approach is the indirect one of obtaining steady-state solutions from time-dependent initial-value problems. This is, of course, a more natural approach since, physically, steady-state flow does not occur spontaneously, but is rather approached as the asymptotic development of a time-dependent process.

While this simple idea is not particularly new, it has only recently begun to receive careful consideration. Crocco (1965) has given an articulate description of the basis for the idea, and used it to calculate the mixed supersonic-subsonic flow in a divergent duct. Also, Bohachevsky, Rubin & Mates (1965) have com-

† Now at the University of Colorado.

puted some non-equilibrium flows with detached shocks, by extending in time suitable non-steady flows. The present paper is an attempt to solve a boundary-layer problem from this viewpoint.

There is, of course, no *a priori* guarantee that the non-steady flow problem will avoid non-linear difficulties; in fact, generally, it will not (the compressible flow problems cited above are both non-linear). However, even in that case, non-steady analysis is still attractive because relatively advanced numerical methods exist for the solution of non-linear initial-value problems (e.g. Richtmyer 1957). On the other hand, the particular time-dependent, initial-value problem studied here, namely, impulsively started boundary-layer flow for an infinite rotating disk, gives rise to linear differential equations, although the forcing functions are non-linear. Moreover, there is evidence that linear equations can arise in more complicated impulsively started boundary-layer problems (Benton 1965).

A major purpose of the present paper, then, is to determine, by reference to an admittedly simple example, whether or not the steady-state boundary-layer problem can actually be approached by way of initial-value analysis and, if so, what sort of difficulties are encountered. In mathematical terms, we seek the rate of convergence of an impulsively started boundary layer to its asymptotic steady state. The question is important because even though there is no conceptual difficulty in approaching the steady state via the initial-value method, the convergence may well be so slow that, analytically, the method is as unwieldy as the direct steady-state approach.

The von Kármán rotating disk problem has been chosen for this study because its velocity field is fully three dimensional (and therefore somewhat general) and the steady-state solution can be obtained very accurately. Also, it reduces to a problem in one variable, which simplifies the details of the analysis very considerably. A special feature of the problem is the well-known fact that the Navier–Stokes equations become identical to the boundary-layer equations for this geometry.

A secondary motivation of the work is to develop a formally exact solution of the time-dependent Navier-Stokes equations and to examine the resulting transient motion. The solution is exact in the sense implied by Schlichting (1960): all terms in the Navier–Stokes equations either vanish identically or are accounted for; none are neglected *a priori*. Formal power-series expansions in Ωt are introduced for the velocity field and pressure and substituted into the full Navier–Stokes equations. When the combined coefficient of each power of Ωt is equated to zero, a relatively simple hierarchy of equations emerges. They are linear ordinary differential equations with variable coefficients and non-linear forcing functions. Since the equations are uncoupled, they can, in principle, be solved exactly in closed form. However, the complexity of the forcing functions increases rapidly with order in the sequence, so only the first four equations are solved exactly. The next six are solved by writing the solutions exactly in integral form, and then evaluating the integrals numerically. At least three terms in each of the series for the velocity field are computed. This enables us to give a fairly complete description of the transient flow and establish to what extent the steady state can be obtained from the initial-value analysis.

2. Basic equations

Non-steady, axially-symmetric, incompressible flow of a homogeneous fluid satisfies the continuity and Navier–Stokes equations in the form

$$(ru)_r + (rw)_z = 0, \tag{1}$$

$$u_t + uu_r + wu_z - r^{-1}v^2 = -\rho^{-1}p_r + \nu[u_{rr} + (r^{-1}u)_r + u_{zz}], \tag{2}$$

$$v_t + uv_r + r^{-1}uv + wv_z = \nu[v_{rr} + (r^{-1}v)_r + v_{zz}], \tag{3}$$

$$w_t + uw_r + ww_z = -\rho^{-1}p_z + \nu[w_{rr} + r^{-1}w_r + w_{zz}]. \tag{4}$$

Here u, v, w are velocity components in the directions of increasing r, θ, z, respectively, in a non-rotating cylindrical co-ordinate system; p is the pressure, ρ the fluid density and ν the kinematic viscosity. Appropriate initial and boundary conditions for the flow induced by an infinite disk ($z = 0$) which is started impulsively (at $t = 0$) into steady rotation with constant angular velocity, Ω, are given by

$$\left.\begin{aligned} &\text{at} \quad t = 0: \quad u = v = w = 0, \\ &\text{at} \quad z = 0: \quad u = w = 0, \quad v = r\Omega, \\ &\text{as} \quad z \to \infty: \quad u, v \to 0. \end{aligned}\right\} \tag{5}$$

Before proceeding to the non-steady analysis, we present, briefly, an improved steady-state solution.

3. Improved steady-state solution

Von Kármán's (1921) original momentum-integral solution to this problem contained errors which were pointed out by Cochran (1934). Cochran reformulated the fifth-order system as a singular-perturbation problem. A power-series solution was found satisfying boundary conditions at the disk. The asymptotic expansion, satisfying boundary conditions at infinity, was shown to consist of power series of exponential functions. These two solutions were joined together at a suitable intermediate point of overlap. The joining process required evaluating a set of five parameters so as to best satisfy five patching conditions. It is remarkable that Cochran was able to obtain as accurate a solution as he did, working without a high-speed computer; yet, two of the functions to be joined mismatch at his patching point by errors slightly over 1 %. Therefore, inaccuracies of that same order may be present throughout his solution. Later in this paper it becomes necessary to know the steady-state solution with greater precision. A highly accurate solution is obtained by a method differing only in trivial respects from one used by Fettis (1955). The essential point is that the asymptotic expansion can be used to describe the entire flow field. In this way the joining difficulties of Cochran's procedure are avoided; furthermore, the new solution is analytically and numerically more convenient for such things as stability investigations.

The von Kármán functional form for the velocity field and pressure is

$$\left.\begin{aligned} u(r,z) &= r\Omega F(\zeta), \quad w(z) = (\nu\Omega)^{\frac{1}{2}} H(\zeta), \\ v(r,z) &= r\Omega G(\zeta), \quad p(z) = -\rho\nu\Omega P(\zeta), \end{aligned}\right\} \tag{6}$$

where

$$\zeta = (\Omega/\nu)^{\frac{1}{2}} z.$$

With these definitions, equations (1)–(4) take on the well-known form

$$H' + 2F = 0, \tag{7}$$

$$F''' - HF' - F^2 + G^2 = 0, \tag{8}$$

$$G'' - HG' - 2FG = 0, \tag{9}$$

$$P' - HH' + H'' = 0. \tag{10}$$

The boundary conditions are

$$G(0) = 1, \quad F(0) = H(0) = G(\infty) = F(\infty) = 0. \tag{11}$$

If P_0 is the dimensionless pressure at $z = 0$, then integration of equation (10) gives

$$P(\zeta) = P_0 + \tfrac{1}{2}H^2 - H'. \tag{12}$$

Substitution of the continuity equation (7) into (8) and (9) leads to the following alternative boundary-value problem:

$$G'' - HG' + H'G = 0, \tag{13}$$

$$H''' - HH'' + \tfrac{1}{2}H'H' - 2G^2 = 0, \tag{14}$$

$$G(0) = 1, \quad H(0) = H'(0) = G(\infty) = H'(\infty) = 0. \tag{15}$$

As $\zeta \to \infty$, there is a finite flow towards the disk, and following Cochran (1934) we define c by

$$H(\infty) = -c \quad (c > 0). \tag{16}$$

Cochran indicated that a formal asymptotic expansion (for large ζ) of the system of equations (13)–(15) is a power series in $\exp(-c\zeta)$, i.e.

$$\left.\begin{aligned} G &\sim A_1 e^{-c\zeta} + A_2 e^{-2c\zeta} + A_3 e^{-3c\zeta} + \ldots, \\ H &\sim -c + B_1 e^{-c\zeta} + B_2 e^{-2c\zeta} + B_3 e^{-3c\zeta} + \ldots. \end{aligned}\right\} \tag{17}$$

This suggests making the change of variable

$$\lambda = e^{-c\zeta}. \tag{18}$$

If $G(\zeta)$ and $H(\zeta)$ are redefined in terms of λ as follows,

$$G(\zeta) = c^2 g(\lambda), \quad H(\zeta) = -c + ch(\lambda), \tag{19}$$

then equations (13), (14) become

$$\lambda g'' + hg' - h'g = 0, \tag{20}$$

$$\lambda^3 h''' + 2\lambda^2 h'' + \lambda^2 hh'' + \lambda hh' - \tfrac{1}{2}\lambda^2 h'h' + 2g^2 = 0, \tag{21}$$

subject to boundary conditions

$$c^2 g(1) = 1, \quad g(0) = h(0) = h'(1) = 0, \quad h(1) = 1. \tag{22}$$

In these equations primes indicate differentiation with respect to λ. The first boundary condition in equation (22) gives c once $g(\lambda)$ has been found. The system of equations (20), (21) can easily be solved completely by power-series expansions in λ. One important advantage of the change of variable is that the region of interest is $0 \leqslant \lambda \leqslant 1$ rather than $0 \leqslant \zeta \leqslant \infty$; so the power series in λ can be

expected to converge more rapidly than one in ζ. With the satisfaction of the boundary conditions at $\lambda = 0$ (i.e. $\zeta \to \infty$), the power series for g and h are

$$g(\lambda) = a_1\lambda + a_2\lambda^2 + a_3\lambda^3 + \ldots \doteq \sum_{i=1}^{n} a_i \lambda^i, \tag{23}$$

$$h(\lambda) = b_1\lambda + b_2\lambda^2 + b_3\lambda^3 + \ldots \doteq \sum_{j=1}^{n} b_j \lambda^j. \tag{24}$$

Recursion relations for the coefficients a_i and b_j are found by substituting the truncated power series into the differential equations (20), (21) and equating the coefficient of the general term to zero. The results can be written

$$a_i = \frac{1}{i(i-1)} \sum_{k=1}^{i-1} (i-2k)\, a_k b_{i-k} \quad (i = 2, 3, 4, \ldots, n), \tag{25}$$

$$b_j = \frac{-1}{2j^2(j-1)} \sum_{k=1}^{j-1} [(j-k)(2j-3k)\, b_k b_{j-k} + 4a_k a_{j-k}] \quad (j = 2, 3, 4, \ldots, n). \tag{26}$$

The first few derived coefficients are

$$\left.\begin{aligned} a_2 &= 0, & b_2 &= -\tfrac{1}{8}(b_1^2 + 4a_1^2), \\ a_3 &= \tfrac{1}{6}(a_1 b_2 - a_2 b_1), & b_3 &= -\tfrac{1}{18}(3b_1 b_2 + 4a_1 a_2), \\ a_4 &= \tfrac{1}{6}(a_1 b_3 - a_3 b_1), & b_4 &= -\tfrac{1}{48}(7b_1 b_3 + 4a_1 a_3 + 2b_2^2 + 4a_2^2). \end{aligned}\right\} \tag{27}$$

Clearly, all of the coefficients can be found exactly as functions of the two leading coefficients, a_1, b_1, which must be chosen so as to satisfy the two remaining boundary conditions [$h(1) = 1, h'(1) = 0$].

Initial guesses for a_1 and b_1 were obtained from Cochran's solution. The recursion relations, equations (25), (26), were then used to compute $a_2, a_3, \ldots, a_{50}, b_2, b_3, \ldots, b_{50}$. Higher-order coefficients can easily be found, but fifty is more than sufficient for the present purpose. The values of $h(1)$ and $h'(1)$ were next calculated from the truncated power series and compared with the desired values (1 and 0, respectively). Then a search process was set up so that a_1 and b_1 would be progressively altered by small amounts until the boundary conditions at $\lambda = 1$ were satisfied with sufficient accuracy.

All computations were made in double precision, thereby ensuring five or six significant digits of accuracy. No more than four digits are presented in the results. The series converge rapidly for two reasons. First, the range of interest is bounded above by $\lambda = 1$. Secondly, the series for h turns out to be an alternating series with coefficients whose magnitudes decrease monotonically. The series for g is almost an alternating series (only a_{23} and a_{24} have the same sign instead of alternating in sign) and, except for two coefficients in the first 50, the magnitudes decrease monotonically.

The final case computed in detail corresponds to the following set of constants:

$$\left.\begin{aligned} &a_1 = 1{\cdot}53678, \quad b_1 = 2{\cdot}36449, \\ \text{for which} \\ &c = 0{\cdot}88447, \quad h(1) = 0{\cdot}9999988, \quad h'(1) = -0{\cdot}0000037. \end{aligned}\right\} \tag{28}$$

For comparison, Cochran's value of c is 0·886 and he finds the asymptotic pressure, $P(\infty)-P_0 = \frac{1}{2}c^2$, to be 0·3925, whereas the present value is 0·3911. Retaining fewer terms, Fettis obtained $c = 0{\cdot}8840$ which gives $P(\infty)-P_0 = 0{\cdot}3907$. The boundary-layer displacement thickness required later is given by

$$d = \left(\frac{\Omega}{\nu}\right)^{\frac{1}{2}}\delta^* = \frac{1}{r\Omega}\int_0^\infty v\,dz = \int_0^\infty G(\zeta)\,d\zeta = 1{\cdot}27144. \tag{28a}$$

To save space, only the first 25 coefficients are tabulated to four significant digits, in table 1. The last two coefficients computed were $a_{50} = -2{\cdot}946\times10^{-12}$, $b_{50} = -7{\cdot}583\times10^{-13}$. The functions originally tabulated by Cochran and recalculated here are presented in table 2. With one exception, the present results, if

i	a_i	b_i
0	0	0
1	1·537 (0)	2·364 (0)
2	0	−1·880 (0)
3	−4·814 (−1)	7·408 (−1)
4	3·795 (−1)	−3·410 (−1)
5	−2·584 (−1)	1·790 (−1)
6	1·657 (−1)	−9·957 (−2)
7	−1·023 (−1)	5·675 (−2)
8	6·128 (−2)	−3·262 (−2)
9	−3·572 (−2)	1·877 (−2)
10	2·032 (−2)	−1·078 (−2)
11	−1·131 (−2)	6·161 (−3)
12	6·163 (−3)	−3·508 (−3)
13	−3·292 (−3)	1·989 (−3)
14	1·724 (−3)	−1·123 (−3)
15	−8·846 (−4)	6·320 (−4)
16	4·438 (−4)	−3·547 (−4)
17	−2·170 (−4)	1·986 (−4)
18	1·028 (−4)	−1·109 (−4)
19	−4·666 (−5)	6·187 (−5)
20	1·990 (−5)	−3·446 (−5)
21	−7·634 (−6)	1·918 (−5)
22	2·312 (−6)	−1·066 (−5)
23	−2·063 (−7)	5·925 (−6)
24	−4·839 (−7)	−3·291 (−6)
25	5·996 (−7)	1·827 (−6)

TABLE 1. The first twenty-five coefficients in the series for the steady-state flow, with exponents of 10 in parentheses

rounded to three places, differ from Cochran's only in the third digit after the decimal point. The largest proportional error occurs at the largest value of ζ, where, for example, Cochran obtains $G(4{\cdot}4) = 0{\cdot}024$ and the present solution gives $G(4{\cdot}4) = 0{\cdot}00245$, a difference of 2 %. Cochran's value for $G(1)$, which is 0·468, must be a misprint, since the more accurate value is 0·477.

ζ	F	G	H	F'	G'	$P-P_0$
0	0	1·0000	0	0·5102	−0·6159	0
0·1	0·0462	0·9386	−0·0048	0·4163	−0·6112	0·0925
0·2	0·0836	0·8780	−0·0179	0·3380	−0·5987	0·1674
0·3	0·1133	0·8190	−0·0377	0·2620	−0·5803	0·2274
0·4	0·1364	0·7621	−0·0628	0·1999	−0·5577	0·2747
0·5	0·1536	0·7076	−0·0919	0·1467	−0·5321	0·3115
0·6	0·1660	0·6557	−0·1239	0·1015	−0·5047	0·3396
0·7	0·1742	0·6067	−0·1580	0·0635	−0·4764	0·3608
0·8	0·1789	0·5605	−0·1934	0·0317	−0·4476	0·3764
0·9	0·1807	0·5171	−0·2294	0·0056	−0·4191	0·3877
1·0	0·1802	0·4766	−0·2655	−0·0157	−0·3911	0·3955
1·1	0·1777	0·4389	−0·3013	−0·0327	−0·3641	0·4008
1·2	0·1737	0·4038	−0·3365	−0·0461	−0·3381	0·4041
1·3	0·1686	0·3712	−0·3707	−0·0564	−0·3133	0·4059
1·4	0·1625	0·3411	−0·4038	−0·0640	−0·2898	0·4066
1·5	0·1559	0·3132	−0·4357	−0·0693	−0·2677	0·4066
1·6	0·1487	0·2875	−0·4661	−0·0728	−0·2470	0·4061
1·7	0·1414	0·2638	−0·4952	−0·0747	−0·2276	0·4053
1·8	0·1338	0·2419	−0·5227	−0·0754	−0·2095	0·4043
1·9	0·1263	0·2218	−0·5487	−0·0751	−0·1927	0·4031
2·0	0·1189	0·2033	−0·5732	−0·0739	−0·1771	0·4020
2·1	0·1115	0·1864	−0·5962	−0·0721	−0·1627	0·4008
2·2	0·1045	0·1708	−0·6178	−0·0698	−0·1494	0·3998
2·3	0·0976	0·1565	−0·6380	−0·0671	−0·1371	0·3987
2·4	0·0910	0·1433	−0·6569	−0·0643	−0·1258	0·3978
2·5	0·0848	0·1313	−0·6745	−0·0612	−0·1153	0·3970
2·6	0·0788	0·1202	−0·6908	−0·0580	−0·1057	0·3962
2·7	0·0732	0·1101	−0·7060	−0·0548	−0·0969	0·3955
2·8	0·0678	0·1008	−0·7201	−0·0517	−0·0888	0·3949
2·9	0·0628	0·0923	−0·7332	−0·0485	−0·0814	0·3944
3·0	0·0581	0·0845	−0·7452	−0·0455	−0·0745	0·3939
3·1	0·0537	0·0774	−0·7564	−0·0425	−0·0683	0·3935
3·2	0·0496	0·0708	−0·7668	−0·0397	−0·0625	0·3932
3·3	0·0458	0·0649	−0·7763	−0·0369	−0·0573	0·3929
3·4	0·0422	0·0594	−0·7851	−0·0343	−0·0524	0·3926
3·5	0·0389	0·0544	−0·7932	−0·0319	−0·0480	0·3924
3·6	0·0358	0·0498	−0·8007	−0·0296	−0·0440	0·3922
3·7	0·0330	0·0456	−0·8075	−0·0274	−0·0403	0·3921
3·8	0·0304	0·0417	−0·8139	−0·0253	−0·0369	0·3919
3·9	0·0279	0·0382	−0·8197	−0·0234	−0·0337	0·3918
4·0	0·0257	0·0349	−0·8251	−0·0216	−0·0309	0·3917
4·1	0·0236	0·0320	−0·8300	−0·0200	−0·0283	0·3916
4·2	0·0217	0·0293	−0·8345	−0·0184	−0·0259	0·3915
4·3	0·0199	0·0268	−0·8387	−0·0170	−0·0237	0·3915
4·4	0·0183	0·0245	−0·8425	−0·0156	−0·0217	0·3914
∞	0	0	−0·8845	0	0	0·3911

TABLE 2. The steady-state velocity field, its derivatives, and the pressure as functions of ζ

4. The impulsively started initial-value problem

In part of the Göttingen thesis, Thiriot (1940) made a start on exactly this problem. He expanded u and v in series involving powers of the angle of disk rotation

$$\phi \equiv \Omega t, \tag{29}$$

with coefficients that were functions of the familiar similarity variable,

$$\eta \equiv z/2(\nu t)^{\frac{1}{2}}. \tag{30}$$

Noting that the steady-state von Kármán radial dependence is equally valid for non-steady flow, and generalizing Thiriot's expansion scheme to include all three velocity components and the pressure, we write

$$u(r,z,t) = r\Omega\phi[f_1(\eta) + f_2(\eta)\,\phi^2 + f_3(\eta)\,\phi^4 + \ldots], \tag{31}$$

$$v(r,z,t) = r\Omega[g_1(\eta) + g_2(\eta)\,\phi^2 + g_3(\eta)\,\phi^4 + g_4(\eta)\,\phi^6 + \ldots], \tag{32}$$

$$w(z,t) = -4(\nu\Omega)^{\frac{1}{2}}\,\phi^{\frac{3}{2}}[h_1(\eta) + h_2(\eta)\,\phi^2 + h_3(\eta)\,\phi^4 + \ldots], \tag{33}$$

$$p(z,t) = 2\rho\nu\Omega\phi[p_1(\eta) + p_2(\eta)\,\phi^2 + p_3(\eta)\,\phi^4 + \ldots]. \tag{34}$$

Before explaining the reasons for choosing these series, we note that Thiriot (1940) found f_1, g_1, and h_1 exactly in closed form, and g_2 by numerical integration. Unfortunately, a numerical error in his equation that determines g_2 vitiates his results for that function. Subsequently, Nigam (1951), apparently unaware of Thiriot's paper (in German), treated the problem and found f_1, g_1, h_1 and p_1 exactly in closed form. In the present paper, g_2 is also found exactly in closed form, and f_2, f_3, g_3, g_4, h_2, and h_3 are calculated by numerical integration (the place of truncation being determined by limitations of machine storage).

We can now explain the reasons for our choice of the above series, a matter not discussed in Thiriot's paper. Since this flow is simply the rotational analogue of the Rayleigh problem, we anticipate a similar solution for v as a first approximation, whence $v_1(r,z,t) = r\Omega g_1(\eta)$ where $\eta = z/2(\nu t)^{\frac{1}{2}}$. In fact, it will be seen that $g_1(\eta)$ for this problem is identical with the solution of the Rayleigh problem (e.g. Schlichting 1960). The crucial difference between the two flows is, of course, that here a v component of velocity is circumferential not rectilinear, so that it produces centrifugal forces, v^2/r. These accelerate a radial secondary flow, u, starting from rest, which for small Ωt must be of order $r\Omega^2 t = r\Omega\phi$ (see equation (2)). Thus, $u_1(r,z,t) = r\Omega\phi f_1(\eta)$. Finally, because of continuity, radial outflow must be accompanied by axial inflow. Substitution of the first approximation to u into the continuity equation (1) shows that $w_1(z,t) = -4(\nu\Omega)^{\frac{1}{2}}\,\phi^{\frac{3}{2}}h_1(\eta)$, as in equation (33). The form of p_1 then follows from equation (4).

It is now evident that similarity is imbedded as the first term in each series in the sense that first approximations f_1, g_1, h_1 and p_1 are functions of only one variable η, with time not appearing explicitly. Departure from similarity is due entirely to the non-linear terms in the differential equations (recall that the Rayleigh problem, which exhibits complete similarity for all time, is fully linear). This departure is accounted for by higher-order terms in the series; these proceed in powers of ϕ^2 rather than ϕ because the non-lincarity is a quadratic one. This feature is fortunate because it prolongs in time the validity of each approximation. Note also that the generation of the velocity field from rest, as described above, proceeds in an ordered sequence, first v, then u, and finally w (i.e. equations (31)–(33) show that for sufficiently small ϕ, $|v| > u| > |w|$). This property leads to linear uncoupled equations for the functions f, g, h. The central purpose of the present paper can now be stated as the examination of the convergence properties

of the above series. If the evolution time for this flow turns out to be of order Ω^{-1} then we can anticipate that the chosen expansion will converge rapidly to the steady-state solution.

Substitution of the series expansions into the full continuity and Navier–Stokes equations (1)–(4) leads to the following hierarchy of equations for $g_1, \ldots, g_4$, $f_1, \ldots, f_3, h_1, \ldots, h_3, p_1, \ldots, p_3$:

$$g_1'' + 2\eta g_1' = 0, \tag{35}$$

$$f_1'' + 2\eta f_1' - 4f_1 = -4g_1^2, \tag{36}$$

$$h_1' = f_1, \tag{37}$$

$$p_1' = -h_1'' - 2\eta h_1' + 6h_1, \tag{38}$$

$$g_2'' + 2\eta g_2' - 8g_2 = 8f_1 g_1 - 8g_1' h_1, \tag{39}$$

$$f_2'' + 2\eta f_2' - 12f_2 = -8g_1 g_2 + 4f_1^2 - 8f_1' h_1, \tag{40}$$

$$h_2' = f_2, \tag{41}$$

$$p_2' = -h_2'' - 2\eta h_2' + 14h_2 - 8h_1 h_1', \tag{42}$$

$$g_3'' + 2\eta g_3' - 16g_3 = 8f_2 g_1 - 8g_1' h_2 + 8f_1 g_2 - 8g_2' h_1, \tag{43}$$

$$f_3'' + 2\eta f_3' - 20f_3 = -4g_2^2 - 8g_1 g_3 + 8f_1 f_2 - 8f_2' h_1 - 8f_1' h_2, \tag{44}$$

$$h_3' = f_3, \tag{45}$$

$$p_3' = -h_3'' - 2\eta h_3' + 22h_3 - 8(h_1 h_2)', \tag{46}$$

$$g_4'' + 2\eta g_4' - 24g_4 = 8(g_3 f_1 - g_3' h_1 + g_2 f_2 - g_2' h_2 + g_1 f_3 - g_1' h_3). \tag{47}$$

The initial and boundary conditions are

$$\left.\begin{aligned} &g_1(0) = 1, \quad g_1(\infty) = 0, \quad g_{i+1}(0) = g_{i+1}(\infty) = 0, \\ &f_i(0) = f_i(\infty) = h_i(0) = 0, \\ &p_1(0) = p_0 = \text{const.}, \quad p_{i+1}(0) = 0, \end{aligned}\right\} \tag{48}$$

for $i = 1, 2, 3$. These linear ordinary differential equations are uncoupled. They can be solved sequentially in the order written, for at any point in the sequence the forcing function consists only of functions previously determined. The equations for the h and p functions require only a single quadrature. The other equations, for the g and f functions, are not quite so straightforward since they have variable coefficients and non-linear forcing functions. Still, all of these latter equations are of the form

$$F_k'' + 2\eta F_k' - 2kF_k = \mathscr{F}_k \quad (k = 0, 2, 4, 6, \ldots, 12), \tag{49}$$

where $F_0(\eta) = g_1(\eta)$, $F_2(\eta) = f_1(\eta)$, $F_4(\eta) = g_2(\eta)$, etc., and $\mathscr{F}_k(\eta)$ is the appropriate forcing function.

As previously anticipated, the solution of equation (35) for the boundary conditions of equation (48) is identical to the solution of the Rayleigh problem

$$g_1(\eta) = \operatorname{erfc}\eta \equiv 2\pi^{-\frac{1}{2}} \int_\eta^\infty e^{-x^2}\, dx. \tag{50}$$

Exact closed form solutions for f_1, h_1, and p_1 (equations (36)–(38)) are given correctly by Nigam (1951) as

$$f_1(\eta) = 2\pi^{-1}[(1+2\eta^2)\operatorname{erfc}\eta - 2\pi^{-\frac{1}{2}}\eta\, e^{-\eta^2}] - 2(\eta\operatorname{erfc}\eta - \pi^{-\frac{1}{2}}e^{-\eta^2})^2, \tag{51}$$

$$\begin{aligned} h_1(\eta) = {} & 2(3\pi)^{-1}[(3\eta+2\eta^3)\operatorname{erfc}\eta - 2\pi^{-\frac{1}{2}}(1+\eta^2)\,e^{-\eta^2}] - \tfrac{2}{3}\eta(\eta\operatorname{erfc}\eta - \pi^{-\frac{1}{2}}e^{-\eta^2})^2 \\ & - \tfrac{2}{3}\pi^{-\frac{1}{2}}e^{-\eta^2}\operatorname{erfc}\eta + \tfrac{2}{3}(2/\pi)^{\frac{1}{2}}\operatorname{erfc}(2^{\frac{1}{2}}\eta) + \tfrac{2}{3}\pi^{-\frac{1}{2}}(2\pi^{-1} - 2^{\frac{1}{2}} + 1), \end{aligned} \tag{52}$$

$$\begin{aligned} p_1(\eta) = {} & (1+2\eta^2)\operatorname{erfc}^2\eta - 4\pi^{-\frac{1}{2}}\eta\, e^{-\eta^2}\operatorname{erfc}\eta - 2\pi^{-1}e^{-2\eta^2} + 4(2/\pi)^{\frac{1}{2}}\eta\operatorname{erfc}(2^{\frac{1}{2}}\eta) \\ & + 4\pi^{-\frac{1}{2}}(2\pi^{-1} - 2^{\frac{1}{2}} + 1)\eta + (2\pi^{-1} - 1 + p_0). \end{aligned} \tag{53}$$

These first terms in the series represent valid approximations to the flow only during the initial stages of motion. They cannot reveal much about the duration or later development of the transient (including the departure from similarity), so it is desirable to obtain higher-order terms. Equations (35)–(47) and (50)–(53) indicate that the complexity of the functions will increase rapidly with order in the sequence. Numerical solution is demanded, but even then the number of higher-order terms that can be calculated accurately is set by limitations of machine storage. The CDC-3600 available for this study could accommodate up to six functions comfortably. These were chosen so that the last function computed would be the fourth approximation to the primary flow, the component of chief interest. As a result, it became necessary to find g_2 exactly in closed form, and also to restrict interest to the velocity field, neglecting pressure. Finding g_2 is a long and tedious process, but it involves a straightforward application of a method due to Goldstein & Rosenhead (1936). The resulting solution to equation (39), with equations (50–52) substituted into the forcing function, is

$$\begin{aligned} g_2(\eta) = {} & [\tfrac{1}{18} + (62 - 27\sqrt{3})/90\pi - 16/15\pi^2][(3+12\eta^2+4\eta^4)\operatorname{erfc}\eta \\ & - 2\pi^{-\frac{1}{2}}(5\eta+2\eta^3)\,e^{-\eta^2}] - \tfrac{1}{18}(3+12\eta^2+28\eta^4)\operatorname{erfc}^3\eta \\ & - \pi^{-1}(1-4\eta^2-4\eta^4)\operatorname{erfc}^2\eta - \tfrac{1}{45}\pi^{-\frac{3}{2}}(53\eta+54\eta^3)\,e^{-3\eta^2} \\ & + (16/3\pi^2)(1+\eta^2)\,e^{-2\eta^2} - (16/15\pi)(2\pi^{-1} - 2^{\frac{1}{2}} + 1)\,e^{-\eta^2} \\ & + \tfrac{4}{3}\pi^{-\frac{1}{2}}(\eta+4\eta^3)\,e^{-\eta^2}\operatorname{erfc}^2\eta - \tfrac{2}{3}\pi^{-\frac{3}{2}}(15\eta+14\eta^3)\,e^{-\eta^2}\operatorname{erfc}\eta \\ & - 6\pi^{-1}\eta^2\,e^{-2\eta^2}\operatorname{erfc}\eta - (16\sqrt{2}/15\pi)\,e^{-\eta^2}\operatorname{erfc}(2^{\frac{1}{2}}\eta) \\ & + (3\sqrt{3}/10\pi)(3+12\eta^2+4\eta^4)\operatorname{erfc}(3^{\frac{1}{2}}\eta). \end{aligned} \tag{54}$$

Accurate solutions for the remaining velocity functions f_2, h_2, g_3, f_3, h_3 and g_4 are obtained by numerical integration. In this set, h_2 and h_3 are found by a single quadrature, using the trapezoidal rule. The other functions are determined by equation (49), the appropriate boundary conditions being

$$F_k(0) = F_k(\infty) = \tag{55}$$

In order to eliminate truncation error, equation (49) is not approximated by a finite difference equation. Instead, the exact solution is written in integral form by the method of variation of parameters and then the integrals are evaluated numerically. This requires first finding the two linearly independent solutions of the homogeneous version of equation (49). One of these, say $F_k^{(1)}(\eta)$ is simply a

polynomial in η^2 of degree $\frac{1}{2}k$. When normalized so that $F_k^{(1)}(0) = 1$, it can be written as (Thiriot 1940)

$$F_k^{(1)}(\eta) = (\tfrac{1}{2}k)! \sum_{i=0}^{\frac{1}{2}k} \frac{2^i}{(i!)\,(\frac{1}{2}k-i)!\,1.3.5\ldots(2i-1)}\,\eta^{2i}. \tag{56}$$

The first homogeneous solution to equation (40) is

$$f_2^{(1)}(\eta) = F_6^{(1)}(\eta) = \tfrac{1}{15}(15 + 90\eta^2 + 60\eta^4 + 8\eta^6). \tag{57}$$

Since the polynomial solution diverges at infinity, it can only contribute to the particular integral.

Thiriot (1940) gives an expression for the second homogeneous solution to equation (49) but a more compact form is

$$F_k^{(2)}(\eta) = \frac{2^{\frac{1}{2}k}k!}{1.3.5\ldots(k-1)} \int\int \ldots \int \operatorname{erfc}(d\eta)^k. \tag{58}$$

The normalization is again $F_k^{(2)}(0) = 1$. This solution decays to zero at infinity. The multiple integral can easily be handled (by integration by parts). For example,

$$\begin{aligned} f_2^{(2)}(\eta) = F_6^{(2)}(\eta) &= 384 \int\int\int\int\int\int \operatorname{erfc}\eta\,(d\eta)^6 \\ &= \tfrac{1}{15}[(15 + 90\eta^2 + 60\eta^4 + 8\eta^6)\operatorname{erfc}\eta - \pi^{-\frac{1}{2}}(66\eta + 56\eta^3 + 8\eta^5)\,e^{-\eta^2}]. \end{aligned} \tag{59}$$

The Wronskian of $F_k^{(1)}(\eta)$ and $F_k^{(2)}(\eta)$, also needed for the variation-of-parameters solution, is defined by

$$W_k(\eta) = F_k^{(2)}(\eta)\,dF_k^{(1)}(\eta)/d\eta - F_k^{(1)}(\eta)\,dF_k^{(2)}(\eta)/d\eta. \tag{60}$$

For equation (49) it has the simple form

$$W_k(\eta) = C_k\,e^{-\eta^2}, \tag{61}$$

where C_k is a constant.

The exact solution of equation (49) for the boundary conditions of equation (55) can now be written as

$$\begin{aligned} F_k(\eta) = &\left[\int_0^\infty \frac{F_k^{(2)}(\eta)\mathscr{F}_k(\eta)}{W_k(\eta)}\,d\eta\right] F_k^{(2)}(\eta) \\ &- F_k^{(1)}(\eta)\int_\eta^\infty \frac{F_k^{(2)}(\chi)\mathscr{F}_k(\chi)}{W_k(\chi)}\,d\chi - F_k^{(2)}(\eta)\int_0^\eta \frac{F_k^{(1)}(\chi)\,\mathscr{F}_k(\chi)}{W_k(\chi)}\,d\chi. \end{aligned} \tag{62}$$

The first term is the direct contribution of the second homogeneous solution, while the last two terms constitute the particular integral. The integrals appearing here were evaluated numerically, using Simpson's rule, but $F_k^{(1)}(\eta)$, $F_k^{(2)}(\eta)$, and $W_k(\eta)$ were supplied in exact form. Those parts of $\mathscr{F}_k(\eta)$ that were not known exactly in analytic form had been stored numerically on tape during previous computations. In equations (44) and (47) the forcing functions contain terms involving the derivatives of functions only known numerically (f_2', g_3', respectively). To maximize accuracy, these derivatives were not obtained by finite

differencing, but rather by using the exact expression for $F'_k(\eta)$, which is (see equation (62))

$$F'_k(\eta) = \left[\int_0^\infty \frac{F_k^{(2)}(\eta)\,\mathscr{F}_k(\eta)}{W_k(\eta)}\,d\eta\right] dF_k^{(2)}(\eta)/d\eta - [dF_k^{(1)}(\eta)/d\eta]\int_\eta^\infty \frac{F_k^{(2)}(\chi)\,\mathscr{F}_k(\chi)}{W_k(\chi)}\,d\chi - [dF_k^{(2)}(\eta)/d\eta]\int_0^\eta \frac{F_k^{(1)}(\chi)\mathscr{F}_k(\chi)}{W_k(\chi)}\,d\chi. \quad (63)$$

In this equation, the differentiated terms are known exactly in analytic closed form and the integrals are the same as those that appear in the expression for $F_k(\eta)$. Thus, there is no loss in accuracy in passing from $F_k(\eta)$ to $F'_k(\eta)$.

An upper limit of infinity in an integral was replaced by $\eta = 4$. Greater values were found to change the results negligibly. The step size used in numerical integrations was $\Delta\chi = 0{\cdot}00125$ for f_2 and h_2; $0{\cdot}0025$ for g_3; $0{\cdot}005$ for f_3 and h_3; and $0{\cdot}01$ for g_4.

5. Results and discussion

The convergence of the series for the primary flow, equation (32), is conveniently discussed by introducing the two most important gross features of the flow, namely the boundary-layer displacement thickness, $\delta^*(t)$, and the viscous torque on the disk, $T(t)$. As is well-known, these are proportional, respectively, to the integral and derivative of the primary flow velocity profile. With appropriate non-dimensionalization, we write

$$\left.\begin{aligned} d(\phi) &= \left(\frac{\Omega}{\nu}\right)^{\frac{1}{2}}\delta^*(t) = \left(\frac{\Omega}{\nu}\right)^{\frac{1}{2}}\int_0^\infty \frac{v}{r\Omega}\,dz \\ &= 2\phi^{\frac{1}{2}}\int_0^\infty [g_1(\eta)+g_2(\eta)\,\phi^2+g_3(\eta)\,\phi^4+g_4(\eta)\,\phi^6+\ldots]\,d\eta \\ &\doteq d_1\phi^{\frac{1}{2}}+d_2\phi^{\frac{5}{2}}+d_3\phi^{\frac{9}{2}}+d_4\phi^{\frac{13}{2}}, \\ \text{where}\quad d_i &= 2\int_0^\infty g_i(\eta)\,d\eta \quad (i=1,2,3,4). \end{aligned}\right\} \quad (64)$$

If T is the viscous torque on that portion of the infinite disk between $r = 0$ and $r = a$, and if $R = a^2\Omega/\nu$ is the Reynolds number, then the torque coefficient for a disk wetted on both sides, is

$$\left.\begin{aligned} C_T &= \frac{-2T}{\frac{1}{2}\pi\rho a^5\Omega^2} = \frac{-4}{\pi\rho a^5\Omega^2}\int_0^{2\pi}\int_0^a \mu\left(\frac{\partial v}{\partial z}\right)_{z=0} r^2\,dr\,d\theta \\ &= -R^{-\frac{1}{2}}\phi^{-\frac{1}{2}}[g_1'(0)+g_2'(0)\,\phi^2+g_3'(0)\,\phi^4+g_4'(0)\,\phi^6+\ldots] \\ &\doteq R^{-\frac{1}{2}}[k_1\phi^{-\frac{1}{2}}+k_2\phi^{\frac{3}{2}}+k_3\phi^{\frac{7}{2}}+k_4\phi^{\frac{11}{2}}], \\ \text{where}\quad k_i &= -g_i'(0) \quad (i=1,2,3,4). \end{aligned}\right\} \quad (65)$$

The minus sign in the definition of C_T makes it positive since the viscous torque opposes the motion (i.e. $T < 0$). The torque is singular at $t = 0$ because the flow was started impulsively.

The numerical values of the coefficients d_i, k_i are

$$\left.\begin{aligned} d_1 &= 1{\cdot}128, \quad d_2 = -0{\cdot}09378, \quad d_3 = 0{\cdot}01256, \quad d_4 = -0{\cdot}001616, \\ k_1 &= 1{\cdot}128, \quad k_2 = 0{\cdot}1884, \quad k_3 = -0{\cdot}01759, \quad k_4 = 0{\cdot}001797. \end{aligned}\right\} \quad (66)$$

This shows that, to the order calculated, the d_i sequence is an alternating sequence with monotonically decreasing magnitudes, thereby indicating convergence. Furthermore, these coefficients decrease rapidly (by about one order of magnitude per step) so the trend towards convergence is also rapid. Similar remarks apply to the sequence k_i, except that the first coefficient is the same sign as k_2, rather than alternating. This is due to the non-homogeneous boundary condition on $g_1(\eta)$.

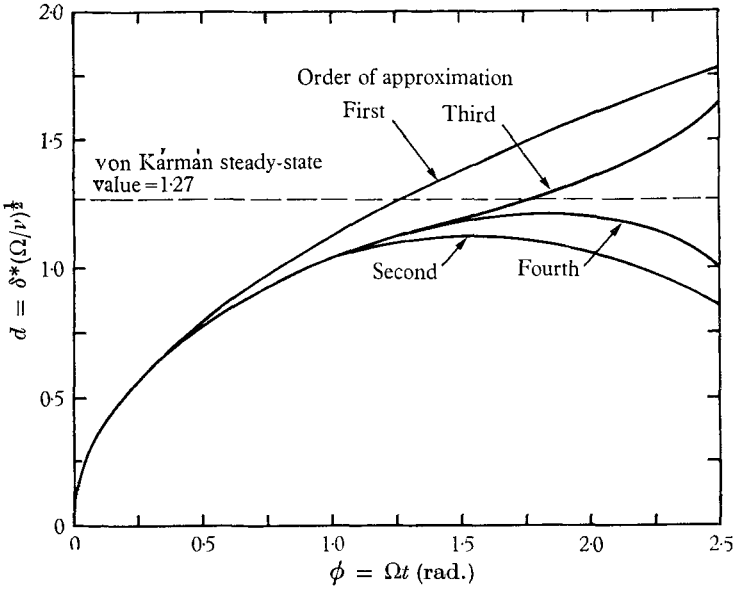

FIGURE 1. Non-dimensional boundary-layer displacement thickness *vs* angle of rotation.

The growth in time of the boundary-layer displacement thickness and viscous torque are shown in figures 1 and 2. The curve for each approximation is the result with only the indicated number of terms in the series included. This allows us to define the range of validity for each approximation by observing where the next higher approximation begins to depart significantly from it (say, by a few per cent). In this way, it is seen that the first approximation, corresponding to a similar solution, extends through about the first half-radian of the disk's motion. The second and third approximations appear to be valid out to about $\phi = 1{\cdot}2$ and 1·7 rad, respectively. The range of validity of the fourth approximation cannot be determined until g_5 is known, but it seems reasonable to extrapolate and assume it valid out to about 1·9 rad. At this point figures 1 and 2 show that the transient solution is close to the steady state. Thus, the evolution time for the flow is of order $\Omega t = 2$ rad. In retrospect, this fact, not previously known, justifies the expansions of the type used in equations (31)–(34) and ensures that only a few terms need be computed.

A very interesting feature of figure 2 is that within the range of validity of the third approximation (specifically, at about $\phi = 1{\cdot}5$ rad) the torque decreases very slightly below the steady-state value. Also, within the assumed validity of the fourth approximation, the torque coefficient goes through a minimum. Thus,

there is a clear suggestion that the ultimate approach to the steady state is not monotonic, but very possibly oscillatory. This is discussed further in the next section. However, it explains the need, met in § 3 of this paper, for a more accurate solution to the steady-state problem than Cochran's solution. The amount of undershoot indicated in figure 2 is only about $2\frac{1}{4}$ %, so errors of that order in the steady-state solution could eliminate it. The accurate steady-state solution revealed errors of that order in Cochran's solution, but his value for the torque is essentially correct. Therefore, the undershoot phenomenon predicted here is believed to be real, not spurious. There is no corresponding overshoot indicated in figure 1.

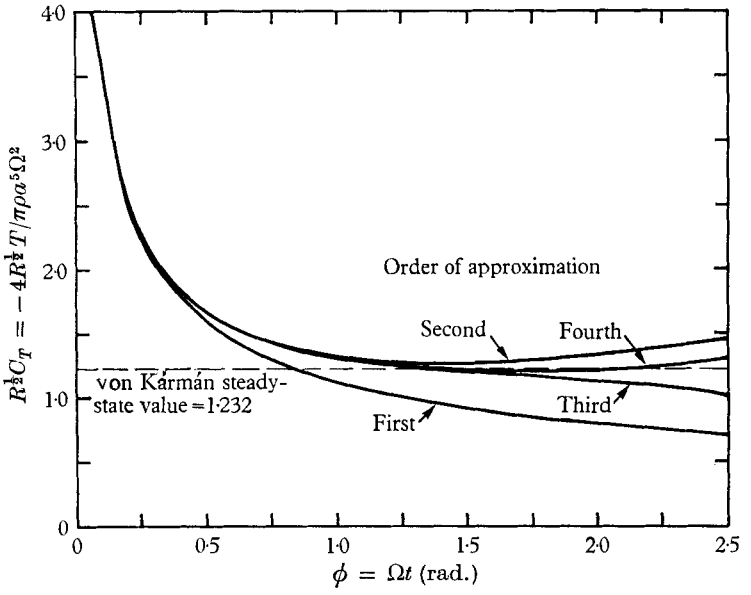

FIGURE 2. Non-dimensional torque *vs* angle of rotation.

The results for the velocity field are given in table 3 where $g_1, g_2, g_3, g_4, f_1, f_2, f_3$, h_1, h_2, h_3 are tabulated as functions of η in steps of $\Delta\eta = 0{\cdot}1$ from $\eta = 0$ to $\eta = 2$. First note that each function is one-signed (the last two entries for g_4 are a measure of round-off error). Secondly, the sequences (g_1, g_2, g_3, g_4), (f_1, f_2, f_3), (h_1, h_2, h_3) are alternating sequences. Finally, if each function is represented by its largest numerical value, then the sequences consist of monotonically decreasing terms, and the rate of decrease is about one order of magnitude per step. These facts again show that, to the order calculated, the series expansions are very well behaved and can describe in considerable detail the non-steady flow throughout the transient period.

Figures 3, 4, 5 show the growth in time of the three velocity profiles towards the steady-state profiles. In these figures the abscissa variable is

$$\zeta = z/\pi^{\frac{1}{2}}\delta^*(\infty) \quad \text{where} \quad \delta^*(\infty) = 1{\cdot}27(\nu/\Omega)^{\frac{1}{2}}$$

is the steady-state boundary-layer displacement thickness. All curves on these figures utilize the most accurate approximation available (i.e. fourth approxima-

η	g_1	g_2	g_3	g_4	f_1	f_2	f_3	h_1	h_2	h_3
0·0	1·00 (−0)	0·00 (−0)	0·00 (−0)	0·00 (−0)	0·00 (−0)	0·00 (−0)	0·00 (−0)	0·00 (−0)	0·00 (−0)	0·00 (−0)
0·1	8·88 (−1)	−1·81 (−2)	1·73 (−3)	−1·79 (−4)	6·37 (−2)	−4·95 (−3)	5·22 (−4)	3·48 (−3)	−2·51 (−4)	2·63 (−5)
0·2	7·77 (−1)	−3·27 (−2)	3·29 (−3)	−3·49 (−4)	9·75 (−2)	−9·11 (−3)	1·00 (−3)	1·18 (−2)	−9·63 (−4)	1·03 (−4)
0·3	6·71 (−1)	−4·24 (−2)	4·53 (−3)	−4·99 (−4)	1·10 (−1)	−1·21 (−2)	1·39 (−3)	2·23 (−2)	−2·03 (−3)	2·23 (−4)
0·4	5·72 (−1)	−4·74 (−2)	5·38 (−3)	−6·18 (−4)	1·08 (−1)	−1·36 (−2)	1·67 (−3)	3·33 (−2)	−3·33 (−3)	3·78 (−4)
0·5	4·80 (−1)	−4·84 (−2)	5·83 (−3)	−6·98 (−4)	9·85 (−2)	−1·40 (−2)	1·82 (−3)	4·37 (−2)	−4·72 (−3)	5·54 (−4)
0·6	3·96 (−1)	−4·66 (−2)	5·92 (−3)	−7·38 (−4)	8·44 (−2)	−1·33 (−2)	1·85 (−3)	5·28 (−2)	−6·09 (−3)	7·38 (−4)
0·7	3·22 (−1)	−4·28 (−2)	5·72 (−3)	−7·41 (−4)	6·92 (−2)	−1·20 (−2)	1·77 (−3)	6·05 (−2)	−7·36 (−3)	9·20 (−4)
0·8	2·58 (−1)	−3·79 (−2)	5·31 (−3)	−7·13 (−4)	5·47 (−2)	−1·03 (−2)	1·61 (−3)	6·67 (−2)	−8·48 (−3)	1·09 (−3)
0·9	2·03 (−1)	−3·26 (−2)	4·77 (−3)	−6·62 (−4)	4·18 (−2)	−8·53 (−3)	1·40 (−3)	7·15 (−2)	−9·42 (−3)	1·24 (−3)
1·0	1·57 (−1)	−2·72 (−2)	4·16 (−3)	−5·95 (−4)	3·11 (−2)	−6·79 (−3)	1·17 (−3)	7·51 (−2)	−1·02 (−2)	1·37 (−3)
1·1	1·20 (−1)	−2·22 (−2)	3·53 (−3)	−5·20 (−4)	2·25 (−2)	−5·24 (−3)	9·46 (−4)	7·78 (−2)	−1·08 (−2)	1·48 (−3)
1·2	8·97 (−2)	−1·78 (−2)	2·93 (−3)	−4·43 (−4)	1·59 (−2)	−3·92 (−3)	7·39 (−4)	7·97 (−2)	−1·12 (−2)	1·56 (−3)
1·3	6·60 (−2)	−1·39 (−2)	2·37 (−3)	−3·67 (−4)	1·10 (−2)	−2·86 (−3)	5·60 (−4)	8·10 (−2)	−1·16 (−2)	1·62 (−3)
1·4	4·77 (−2)	−1·06 (−2)	1·88 (−3)	−2·96 (−4)	7·47 (−3)	−2·03 (−3)	4·13 (−4)	8·20 (−2)	−1·18 (−2)	1·67 (−3)
1·5	3·39 (−2)	−7·94 (−3)	1·46 (−3)	−2·32 (−4)	4·96 (−3)	−1·41 (−3)	2·96 (−4)	8·26 (−2)	−1·20 (−2)	1·71 (−3)
1·6	2·37 (−2)	−5·83 (−3)	1·11 (−3)	−1·74 (−4)	3·23 (−3)	−9·57 (−4)	2·08 (−4)	8·30 (−2)	−1·21 (−2)	1·73 (−3)
1·7	1·62 (−2)	−4·19 (−3)	8·24 (−4)	−1·23 (−4)	2·07 (−3)	−6·37 (−4)	1·42 (−4)	8·32 (−2)	−1·22 (−2)	1·75 (−3)
1·8	1·09 (−2)	−2·96 (−3)	6·00 (−4)	−7·83 (−5)	1·30 (−3)	−4·15 (−4)	9·53 (−5)	8·34 (−2)	−1·22 (−2)	1·76 (−3)
1·9	7·21 (−3)	−2·04 (−3)	4·28 (−4)	−3·74 (−5)	8·01 (−4)	−2·65 (−4)	6·26 (−5)	8·35 (−2)	−1·23 (−2)	1·77 (−3)
2·0	4·68 (−3)	−1·38 (−3)	2·99 (−4)	1·57 (−6)	4·86 (−4)	−1·66 (−4)	4·03 (−5)	8·36 (−2)	−1·23 (−2)	1·77 (−3)
2·5	4·07 (−4)	−1·46 (−4)	3·65 (−5)	2·79 (−4)	3·06 (−5)	−1·23 (−5)	3·26 (−6)	8·37 (−2)	−1·23 (−2)	1·78 (−3)

TABLE 3. The coefficients in the series expansions for the impulsively started velocity field, tabulated as functions of the similarity variable

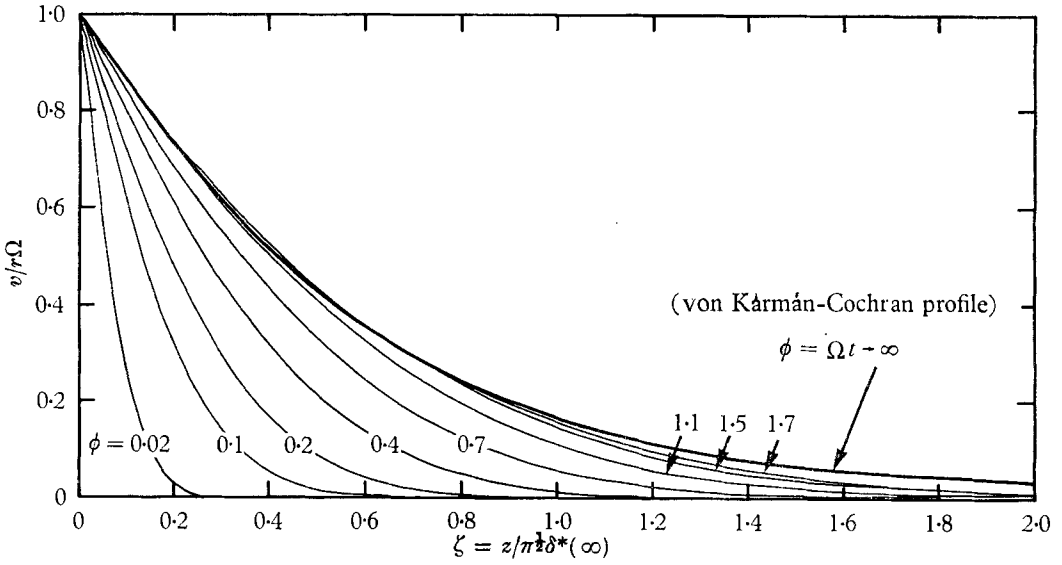

FIGURE 3. Growth of the circumferential flow towards the von Kármán–Cochran steady-state profile.

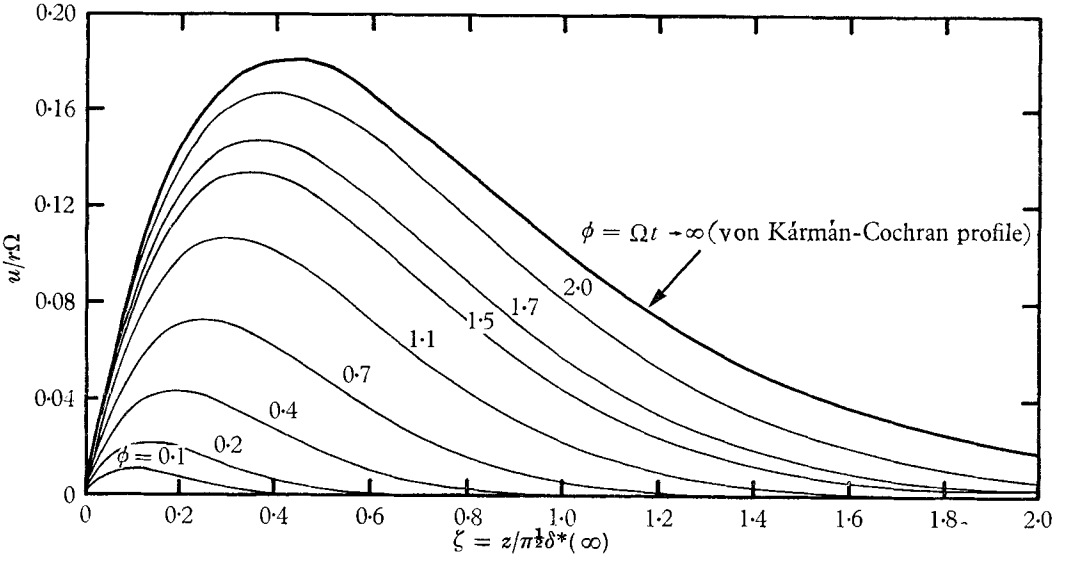

FIGURE 4. Growth of the radial flow towards the von Kármán–Cochran steady-state profile.

tion for figure 3 and third for figures 4 and 5). The curves for $\phi = 2$ rad in figures 4 and 5 are not really reliable since the third approximation has outlived its validity at that time. They are included only to show that the predicted secondary flow profiles are nearly the same shape as the steady-state ones, and also to indicate that the secondary flow lags in its development behind the primary flow (which, apart from overshoot effects which are observable in figure 3, approaches its steady state after only about 1·7 rad).

The flow has three distinct phases. Phase 1, which lasts up to about $\Omega t = 0{\cdot}5$ rad, is characterized by a similar solution (the first terms in the expansions dominate). During this phase, growth in the boundary-layer displacement thickness is the only significant dynamical effect. The shapes of the velocity profiles remain essentially constant (provided we define the shapes by $v/r\Omega$, $u/r\Omega d^2$, $w/(\nu\Omega)^{\frac{1}{2}}d^3$, since $d \sim \phi^{\frac{1}{2}}$). For Ωt between roughly 0·5 and 1·5 rad (phase 2), boundary-layer growth continues, though at a slower rate, and simultaneously, because of the growing importance of the non-linear convective acceleration, the velocity profiles adjust in shape towards the steady-state profiles. Finally, at about $\Omega t = 1{\cdot}5$,

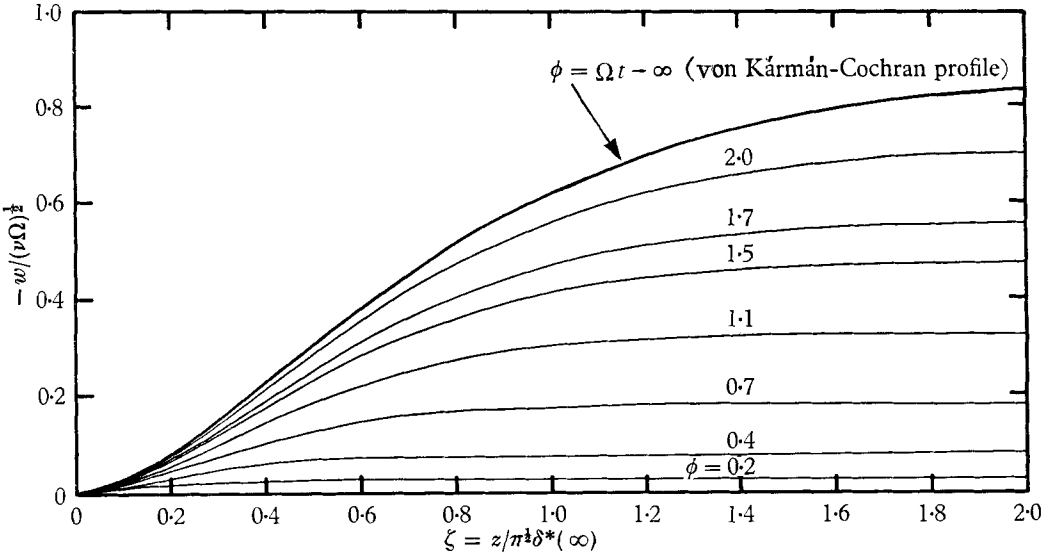

FIGURE 5. Growth of the axial flow towards the von Kármán–Cochran steady-state profile.

the beginning of phase 3, the slope of the primary flow profile at the disk overshoots the steady-state value by a very small amount, clearly indicating that a non-monotonic process (phase 3) must follow. Many more than the available four terms would be required in order to follow in detail the return to the steady state following overshoot. However, in analogy with the 'Greenspan–Howard problem' discussed below, it is surmised that the third phase consists of a small amplitude decaying oscillation, of frequency 2Ω, about the steady state.

6. Relationship to the 'Greenspan–Howard problem'

Greenspan & Howard (1963) have recently presented an interesting analysis of a rotating time-dependent flow to which the present problem is related. In their problem, a general axially symmetric closed container rotates about its axis of symmetry with an angular velocity Ω. The contained fluid is in uniform rotation at the same angular velocity. At time $t = 0$, the angular velocity of the container is impulsively changed by a small amount $\epsilon\Omega$. Their analysis describes in detail the return of the fluid to the new steady-state rigid-body rotation.

As the simple prototype for the general problem, Greenspan & Howard considered a closed container formed by two infinite parallel coaxial disks, separated by a distance $2L$, which rotate in unison. They showed that the transient flow consists of three distinct phases. Phase 1, lasting up to $\Omega t = O(1)$, is the establishment of a quasi-steady Ekman layer on each disk with an inviscid geostrophic region in between. During this period, there is essentially no interaction between the two layers. Consequently, this phase corresponds (apart from the difference in initial condition) to the monotonic growth of the boundary layer in the present problem (our phases 1 and 2). Had Greenspan & Howard analysed their first phase in more detail (which was not their purpose) they probably would have found a subphase of similar flow followed by a subphase of non-similar flow.

The second phase is the important one in the 'Greenspan–Howard problem', but it is absent in the single disk problem. During their phase 2, which lasts up until $t \sim L/(\nu\Omega)^{\frac{1}{2}}$, the angular momentum of the inviscid interior region increases (if $\epsilon > 0$) towards the new steady-state value. This 'spin-up' occurs not by viscous diffusion, but rather because of secondary flow associated with the Ekman layers *and* the geometrical constraint provided by the second disk. This phase has no analogue in the present problem because there is no second disk and therefore no 'spin-up' to a new uniform rotation (our container is not closed).

Their third phase lasts until $t \sim L^2/\nu$. It consists of the final viscous decay of inertial oscillations (at frequency 2Ω) which are excited initially by the impulse. It is suggested that similar oscillations may be excited in the present problem within the fluid rotating in the boundary layer. However, in their paper Greenspan & Howard argue that these oscillations are collectively (as well as individually) unimportant, essentially because the combined amplitude is at most of order $R^{-\frac{1}{2}} = (L^2\Omega/\nu)^{-\frac{1}{2}}$ (refer to their equations (3·9) and (3·10), and the paragraphs that follow, but note there are misprints in those equations). Quantitatively this is correct, but qualitatively it does not seem to be warranted. In fact, Howard (1965, private communication) agrees with the present writer that the ultimate approach to the steady state may well be a small amplitude decaying oscillation about the steady state. This implies that there is overshoot (even though by a small amount) and that the inertial oscillations are of considerable qualitative importance, although quantitatively small. Clearly, whether or not the total solution (steady state, plus monotonic growth, plus inertial oscillations) overshoots the steady state depends upon the ratio of the instantaneous oscillation amplitude to the monotonic growth term. It can easily be shown (appendix 1) that this ratio will certainly exceed 1 in Greenspan & Howard's problem for times of an order greater than $t = \Omega^{-1}R^{\frac{1}{2}}\ln R$ (and possibly sooner). This proves that there is actually overshoot in their problem. In the single disk case there is no Reynolds number to govern the amplitude of inertial oscillations so overshoot may be expected sooner (Greenspan & Howard point out that during the early phase of the motion the inertial oscillation term is comparable in magnitude to the other terms in the solution). In any case, phase 3 of the present problem is believed to correspond to Greenspan & Howard's third phase. However, this clearly needs further study.

The author is indebted to Mr Loren Wagner for the forms of equations (25), (26) and for programming the calculations reported in this paper. Thanks are also due to a referee for calling attention to the important paper by Fettis. The work was supported by the National Science Foundation through its basic contract with the National Center for Atmospheric Research.

REFERENCES

BENTON, E. R. 1965 Laminar boundary layer on an impulsively started rotating sphere. *J. Fluid Mech.* **23**, 611.

BOHACHEVSKY, I. O., RUBIN, E. L. & MATES, R. E. 1965 A direct method for computation of nonequilibrium flows with detached shocks. *AIAA Paper* no. 65–24, presented at the 2nd Aerospace Sciences Meeting, New York, Jan. 25–27, 1965.

COCHRAN, W. G. 1934 The flow due to a rotating disk. *Proc. Camb. Phil. Soc.* **30**, 365–375.

CROCCO, L. 1965 A suggestion for the numerical solution of the steady Navier–Stokes equations. *AIAA J.* **3**, 1824–32.

FETTIS, H. E. 1955 On the integration of a class of differential equations occurring in boundary layer and other hydrodynamic problems. *Proc. 4th Midwestern Conf. on Fluid Mech., Purdue.*

GOLDSTEIN, S. & ROSENHEAD, L. 1936 Boundary layer growth. *Proc. Camb. Phil. Soc.* **32**, 392–401.

GREENSPAN, H. P & HOWARD, L. N. 1963 On a time-dependent motion of a rotating fluid. *J. Fluid Mech.* **17**, 385–404.

VON KÁRMÁN, TH. 1921 Laminare und turbulente reibung. *Z. angew. Math. Mech.* **1**, 244–247.

NIGAM, S. D. 1951 Rotation of an infinite plane lamina: Boundary layer growth: Motion started impulsively from rest. *Quart. Appl. Math.* **9**, 89–91.

RICHTMYER, R. D. 1957 *Difference Methods for Initial-value Problems.* New York: Interscience.

SCHLICHTING, H. 1960 *Boundary Layer Theory,* 4th ed. New York: McGraw-Hill.

THIRIOT, H. K. 1940 Über die laminare Anlaufströmung einer Flüssigkeit einem rotierenden Boden bei plötzlicher Änderung des drehungszustandes. *Z. angew. Math. Mech.* **20**, 1–13.

Appendix 1. Dominance of inertial oscillations in the Greenspan–Howard problem

It can be shown that after a finite time the inertial oscillation term in the Greenspan–Howard problem actually dominates the monotonic growth term, so that overshoot of the steady state is inevitable. In our notation and in an inertial co-ordinate system, the correct version of equation (3.10) in Greenspan & Howard (1963) for the primary flow is

$$\frac{v}{\epsilon r\Omega} = \frac{1+\epsilon}{\epsilon} - \exp(-R^{-\frac{1}{2}}\phi)\,[1-\exp[-R^{\frac{1}{2}}(1-|z|/L)]\cos R^{\frac{1}{2}}(1-|z|/L)] + R^{-1}\sin 2\phi \sum_n \left[\frac{\cos(\xi_n z/L)}{\cos\xi_n} - 1\right]\exp(-\xi_n^2 R^{-1}\phi),$$

where ξ_n is the nth positive roots of $\tan\xi = \xi$, the Reynolds number is $R = L^2\Omega/\nu$, and the z co-ordinate is $+L$ on the top disk and $-L$ on the bottom disk. In this equation, the first term is the final steady-state uniform rotation. The second

term gives the monotonic growth of the Ekman layers, and the third term, the inertial oscillation at frequency 2Ω.

While it is possible to work directly from this equation, it is somewhat simpler to consider the viscous torque on one disk, say the top one. This is proportional to $(\partial v/\partial z)_{z=L}$, which is given by

$$\frac{1}{er\Omega}\left(\frac{\partial v}{\partial z}\right)_{z=L} = R^{\frac{1}{2}}\exp(-R^{-\frac{1}{2}}\phi) - R^{-1}\sin 2\phi \sum_n \xi_n^2 \exp(-\xi_n^2 R^{-1}\phi).$$

If the last term here can be larger in magnitude than the first term on the right, then the viscous torque will overshoot the steady-state value. All terms in the summation here are positive, so it is sufficient to show that there is a value of ϕ such that

$$R^{-1}\xi_1^2 \exp(-\xi_1^2 R^{-1}\phi) > R^{\frac{1}{2}}\exp(-R^{-\frac{1}{2}}\phi),$$

where $\xi_1 \doteq \frac{3}{2}\pi$. This is clearly satisfied if

$$\phi > (1-\xi_1^2 R^{-\frac{1}{2}})^{-1} R^{\frac{1}{2}} \ln(\xi_1^{-2} R^{\frac{3}{2}}).$$

Now since $\xi_1^2 \doteq 19$ and R is to be large, overshoot will certainly occur for values of Ωt greater than $\frac{3}{2}R^{\frac{1}{2}}\ln R$, and probably sooner. It may be noted that $\Omega t = R^{\frac{1}{2}}\ln R$ lies within Greenspan & Howard's second phase.